Available online at www.sciencedirect.com
SCIENCE DIRECT®
International Journal of Thermal Sciences 44 (2005) 1072–1077
International Journal of Thermal Sciences
www.elsevier.com/locate/ijts

Heat transfer enhancement in a vertical annulus by electrophoretic forces acting on a dielectric liquid

Walter Grassi *, Daniele Testi, Mario Saputelli

LOTHAR (LOw gravity and THermal Advanced Research laboratory), Department of Energetics "L. Poggi", University of Pisa, via Diotisalvi 2, 56126 Pisa, Italy

Received 15 November 2004; received in revised form 14 March 2005; accepted 29 March 2005

Available online 6 June 2005

Abstract

In the presence of a sharp HV electrode, free charge can build up in a single-phase liquid by ion injection at the metal/liquid interface. Electrophoretic forces acting on ions can generate strong convective motion, thus augmenting the heat transfer rate.

In a vertical annular duct, uniformly heated on the outer wall, a dielectric liquid is weakly forced to flow upward. Sharp points are added perpendicularly to the inner cylinder and d.c. voltages as high as 22 kV are applied to it, while the outer wall is grounded.

Prior to the application of the electric field, a regime of turbulent aided mixed convection is obtained. Being in a region of thermally developing flow, laminarization effects are observed, with local heat transfer coefficients depending non-trivially on longitudinal position, heat flux, and flow rate.

With the electric field on, heat transfer turns out to be only weakly influenced by the heat flux and the flow rate. The heat exchange reveals to be highly enhanced by this technique and can be modulated by varying the applied voltage. In all cases, the heat transfer improvement is accompanied by a slight increase in pressure drop through the test section and a negligible Joule heating.

Keywords: EHD (electrohydrodynamics); Heat transfer enhancement; Ion injection; Electrophoresis; Mixed convection

1. Introduction

In the presence of an electric field, a dielectric fluid is subjected to body forces, which may readily be expressed as [1]:

$$\mathbf{f}_E = \rho_E \mathbf{E} - \frac{1}{2}E^2\nabla\varepsilon + \frac{1}{2}\nabla\left[\rho E^2\left(\frac{\partial\varepsilon}{\partial\rho}\right)_T\right] \tag{1}$$

Respectively, these forces are commonly identified as electrophoretic (or Coulombic), dielectrophoretic, and electrostrictive. The Coulomb force is exerted by an electric field upon the free charge present in the fluid, while the other two forces act on polarization charges.

In order to solve an electrohydrodynamic (EHD) problem, one needs to insert $\mathbf{f}_E$ in the momentum equation among the external forces. Besides, the complete set of Maxwell equations, together with free charge continuity, is required in addition to the mass, momentum, and energy balances.

The electrostrictive term, being an irrotational one, may be lumped in a modified pressure together with the hydrodynamic one:

$$p_m = p - \frac{1}{2}\nabla\left[\rho E^2\left(\frac{\partial\varepsilon}{\partial\rho}\right)_T\right] \tag{2}$$

Furthermore, in single-phase liquids under d.c. fields, dielectrophoresis can be neglected with respect to the Coulomb force. Free charge can be created in the fluid by three main mechanisms: temperature gradients (which induce electrical conductivity gradients), field-enhanced dissociation of electrolytic species, and ion injection at the electrode/liquid interface via electrochemical reactions. In the presence of a sharp electrode and at d.c. electric fields as

* Corresponding author. Tel.: +39 050 2217090; fax: +39 050 830116.
E-mail address: w.grassi@ing.unipi.it (W. Grassi).

1290-0729/$ – see front matter
doi:10.1016/j.ijthermalsci.2005.03.017

Nomenclature

c_p	specific heat	$\mathrm{J\cdot kg^{-1}\cdot K^{-1}}$
D	inner diameter of the heated wall	m
D_h	$= D - d$, hydraulic diameter	m
d	diameter of the inner wire	m
$\mathbf{E}$	electric field	$\mathrm{V\cdot m^{-1}}$
f	Darcy–Weisbach friction factor	
$\mathbf{f}_E$	electric body force	$\mathrm{N\cdot m^{-3}}$
Gr	$= \frac{\beta g(T_{w\_\mathrm{in}} - T_b)D_h^3}{\nu^2}$, Grashof number	
Gr_h	Grashof number based on the wall heat flux	
Gr_τ	electrophoretic Grashof number	
HV	applied high voltage	V
L_h	heated length	m
$\dot{m}$	$= \rho\dot{V}$, mass flow rate	$\mathrm{kg\cdot s^{-1}}$
Nu	local Nusselt number	
$\langle Nu\rangle$	longitudinal average of the Nusselt number	
p	hydrodynamic pressure	Pa
p_m	modified pressure	Pa
q	heat flux	$\mathrm{W\cdot m^{-2}}$
Re	Reynolds number	
s	heated wall thickness	m
T	temperature	K
$\mathbf{u}$	fluid velocity	$\mathrm{m\cdot s^{-1}}$
$\dot{V}$	volumetric flow rate	$\mathrm{m^3\cdot s^{-1}}$

Greek letters

α	convective heat transfer coefficient	$\mathrm{W\cdot m^{-2}\cdot K^{-1}}$
β	coefficient of cubic expansion	$\mathrm{K^{-1}}$
β_τ	temperature coefficient of relaxation time	$\mathrm{K^{-1}}$
ε	electrical permittivity	$\mathrm{F\cdot m^{-1}}$
η	dynamic viscosity	Pa·s
Λ	heated wall thermal conductivity	$\mathrm{W\cdot m^{-1}\cdot K^{-1}}$
λ	fluid thermal conductivity	$\mathrm{W\cdot m^{-1}\cdot K^{-1}}$
ν	$= \frac{\eta}{\rho}$, kinematic viscosity	$\mathrm{m^2\cdot s^{-1}}$
Π_h	heat flow	W
Π_P	pumping power	W
ρ	mass density	$\mathrm{kg\cdot m^{-3}}$
ρ_E	free charge density	$\mathrm{C\cdot m^{-3}}$
σ	electrical conductivity	$\Omega^{-1}\cdot\mathrm{m^{-1}}$
τ	$= \frac{\varepsilon}{\sigma}$, free charge relaxation time	s

Subscripts

b	bulk
f	calculated at film temperature
in	inlet
out	outlet
w_in	inner side of the heated wall
w_out	outer side of the heated wall

high as 10^7 $\mathrm{V\cdot m^{-1}}$, the latter phenomenon is the dominating one [2,3].

Ion injection is mainly controlled by the high field electrochemistry of the interface, which critically depends on the chemical nature of the dielectric fluid and on the shape (radius of curvature), composition, and polarity of the electrode. If the liquid is a good insulator, its electrochemical properties are determined by the extrinsic ions having electrodonor or electroacceptor qualities.

The phenomenon generally occurs at the sharper electrode only. The injected charges are homocharges [4], i.e: of the same polarity as the injecting electrode, to which we generally refer as the emitter. Fingers of highly charged liquid coming from the boundary layer of the emitter give rise to a jet-like motion towards the facing electrode [5].

The velocities induced in the bulk of the fluid can be assessed, assuming a conversion of electric energy into kinetic energy:

$$\frac{1}{2}\rho u^2 \approx \frac{1}{2}\varepsilon E^2 \implies u \approx E\sqrt{\frac{\varepsilon}{\rho}} \tag{3}$$

In liquids, the induced fluid velocity is higher than the ion drift velocity. Then, the charge distribution depends drastically on the motion it induces.

A high heat transfer enhancement by ion injection can be obtained with fluids of low viscosity and low electrical conductivity [6]. In fact, an increased viscosity of the fluid delays the onset of the electrohydrodynamic motion and the concurrent strong charge injection. Besides, with a high electrical conductivity, the ions in the liquid cross the space between the electrodes before they can thoroughly exchange their momentum with the neutral fluid molecules. This lack of momentum transfer decreases the induced velocity and thus the heat transfer augmentation.

2. Experimental apparatus

In this work we examine the effect of a d.c. electric field on turbulent aided mixed convection in a heated vertical annulus with sharp points added perpendicularly to the inner electrode at various longitudinal locations. According to the map proposed by Metais and Eckert [7], the transition from the laminar to the turbulent regime occurs in the Reynolds number range 200–400.

2.1. The working fluid

The dielectric fluid chosen for the experimental campaign is FC-72, a Fluorinert™ Electronic Liquid. FC-72 is thermally and chemically stable, compatible with sensitive materials, non-flammable, non-toxic, colorless, and has no ozone depletion potential. The physical properties of the fluid at 25 °C are reported in Table 1.

Table 1
FC-72 properties at 25 °C (by courtesy of 3M)

Chemical formula	C_6F_{14}
Electrical conductivity	$10^{-13}\ \Omega^{-1}\cdot m^{-1}$
Dielectric strength	$1.5 \times 10^7\ V\cdot m^{-1}$
Relative permittivity	1.75
Boiling point (at 1 bar)	56 °C
Density	$1.68 \times 10^3\ kg\cdot m^{-3}$
Kinematic viscosity	$3.8 \times 10^{-7}\ m^2\cdot s^{-1}$
Specific heat	$1.1 \times 10^3\ J\cdot kg^{-1}\cdot K^{-1}$
Thermal conductivity	$5.7 \times 10^{-2}\ W\cdot m^{-1}\cdot K^{-1}$
Coefficient of cubic expansion	$1.56 \times 10^{-3}\ K^{-1}$

FC-72 has a low viscosity and an extremely low electrical conductivity, thus being really suitable for EHD processes. Moreover, the low viscosity of FC-72 is very attractive also from a purely hydraulic point of view. In fact, in a pipe of length L and cross section area A, the pumping power needed to compensate for pressure drop, at a given Reynolds number, can be expressed as:

$$\Pi_P = \dot{V}\,\Delta p = \frac{1}{2}\rho A \frac{Re^3\nu^3}{D_h^3} f \frac{L}{D_h} = \chi\rho\nu^3 \tag{4}$$

being χ dependent only on geometrical parameters and on the Reynolds number. Thus, it must be taken into account that a reduction in viscosity can greatly diminish the required pumping power.

2.2. Description of the apparatus

A test loop was built as shown in the schematic of Fig. 1. The fluid, moved by a peristaltic pump, circulated through the test specimen at volumetric flow rates in the range 0.25–1.00 lt·min^{-1}. An asameter measured the flow rate with an accuracy of ±0.011 lt·min^{-1}. The fluid, uniformly heated in its upward flow along the test section, was cooled to the desired inlet temperature by means of a shell-tube heat exchanger, with countercurrent chilled water flowing in the shell. The annular test specimen was connected either with a 0–30 kV d.c. positive high voltage power supply, or with a 0–10 kV d.c. reversible polarity one. An expansion vessel was used to compensate the volume increase in the loop due to temperature variations and to set the pressure of the position it was mounted on. An absolute pressure transducer was placed right upstream of the peristaltic pump, in order to check that the lowest pressure of the loop was above the room pressure, thus avoiding air from being sucked in by the pump. All the tests were performed at an absolute pressure of about 2 bars.

A detailed schematic of the test section is shown in Fig. 2. The inner wire, of diameter $d = 1.6$ mm, was made of stainless steel. The outer electrode, also made of stainless steel, had an inner diameter $D = 17$ mm and a wall thickness $s = 2$ mm. The fluid was warmed up by an electrical resistance heater applied to the outer wall for a length $L_h = 500$ mm. 20 thermocouples were placed on the outer wall, under the

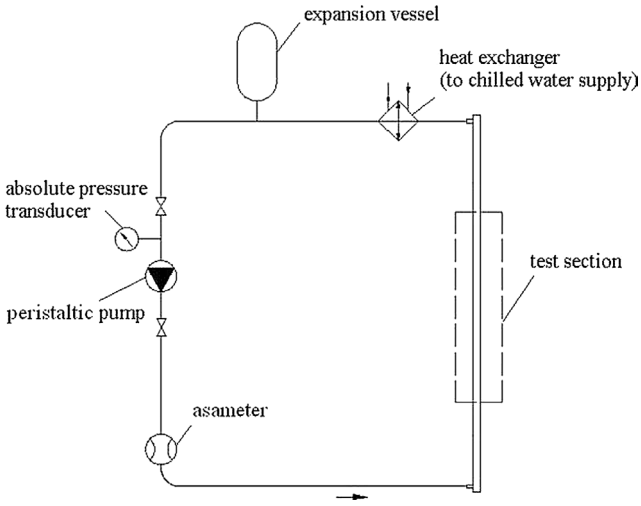

Fig. 1. Schematic of the test loop.

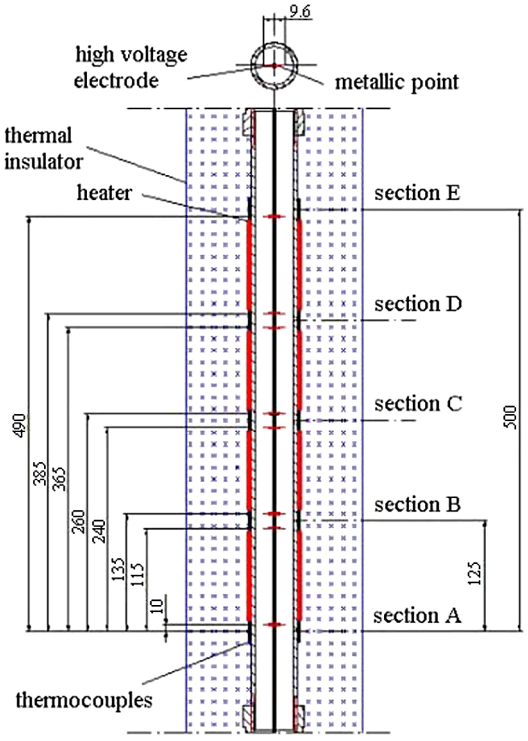

Fig. 2. Detail of the EHD test section in configuration 1 (distances are expressed in mm).

heater, at five cross sections, 125 mm apart along the heated length. Each section had four thermocouples, one every 90°. To minimize heat losses, the entire specimen was covered with a thermal insulator ($\lambda = 0.038\ W\cdot m^{-1}\cdot K^{-1}$). Two more thermocouples were placed at the fluid inlet and outlet, to evaluate the heat flow supplied to the test section in steady state through the energy balance:

$$\Pi_h = \dot{m} c_p (T_{out} - T_{in}) \tag{5}$$

having assumed that the electrically generated heat within the fluid is negligible, since we never measured currents higher than 10^{-6} A.

All the thermocouples were type-T and used a zero-point reference cell, whose temperature was controlled by a reference resistance thermometer. The overall accuracy of each thermocouple after calibration in the 15–60 °C range was ±0.3 K.

A differential pressure transducer measured the pressure drop through the test section. At the application of the electric field, we could not appreciate order of magnitude variations in the pressure drop, with measured values below 10 Pa.

Metallic points were welded perpendicularly to the inner electrode by means of a silver alloy. The points were simply tin-coated copper wires, of diameter 0.6 mm and length 4 mm, sharply cut at the tip with an angle of about 45°.

In a first series of tests, to which we shall refer as configuration 1, two opposite points were placed at each of the longitudinal locations showed in Fig. 2. Further tests (configuration 2) were conducted with no points at section C and with two additional opposite points located 40 mm upstream of section A, thus in an unheated region.

2.3. Test procedure and data analysis

In a preliminary operation, we tested the dielectric strength of the medium. Slowly increasing the applied voltage, we observed that electrical breakdown occurred at 24 kV. Therefore, we decided not to operate above $HV = 22$ kV.

Every test was run under constant volumetric flow rate and heat flow and a steady state condition was awaited, with or without the electric field. The thermocouples' signals were acquired every 6 seconds by a scanner mounted on a digital multimeter; then the data were sent to a PC in order to be recorded and processed.

The bulk temperature of the fluid at a given axial position was calculated considering a temperature of adiabatic mixing for the examined cross section, assuming a linear trend, from the inlet to the outlet temperature, on the heated length. The temperatures of the inner side of the wall were obtained from the ones measured on the outer side, properly accounting for one-dimensional heat conduction within the wall thickness:

$$T_{w\_\mathrm{in}} = T_{w\_\mathrm{out}} - \frac{\Pi_h}{2\pi \Lambda L_h} \ln\left(\frac{D+2s}{D}\right) \tag{6}$$

The dimensionless numbers describing mixed convection in uniform heat flux conditions (i.e.: *Nu*, *Re*, and Gr_h) were calculated as:

$$\begin{cases} Nu = \frac{\alpha D_h}{\lambda_f} = \frac{q D_h}{\lambda_f (T_{w\_\mathrm{in}} - T_b)} = \frac{\Pi_h}{\lambda_f (T_{w\_\mathrm{in}} - T_b)\pi L_h} \\ Re = \frac{u \rho_{\mathrm{in}} D_h}{\eta_{\mathrm{in}}} = \frac{4\dot{V}}{\pi (D+d) \nu_{\mathrm{in}}} \\ Gr_h = Gr\, Nu = \frac{\beta_{\mathrm{in}} g q D_h^4}{\lambda_{\mathrm{in}} \nu_{\mathrm{in}}^2} = \frac{\beta_{\mathrm{in}} g \Pi_h D_h^3}{\lambda_{\mathrm{in}} \nu_{\mathrm{in}}^2 \pi L_h} \end{cases} \tag{7}$$

The maximum relative error on the Nusselt number, corresponding to the highest heat transfer rate and the lowest heat flow, was 11.3%.

Even at the highest heat flow, the fluid temperatures in correspondence of the inner side of the heated wall were fairly below the boiling point, never exceeding 50 °C.

3. Discussion of heat transfer results

In every test, the data were obtained averaging 20 measurements recorded consecutively once a steady state condition was reached. The local Nusselt number values (*Nu*) represent the azimuthal average on the examined cross section. The longitudinal average of *Nu*, which expresses the overall performance of the heated test section, is indicated as $\langle Nu \rangle$.

In Fig. 3 $\langle Nu \rangle$ is plotted against *Re* at three different Gr_h and at $HV = 0$, 18.5, and 22 kV; the metallic points are placed in configuration 1.

Without the electric field, $\langle Nu \rangle$ increases with Gr_h and slightly decreases with an increase in *Re*.

In a regime of turbulent aided mixed convection, laminarization may occur along the heated length, penalizing the heat transfer, and this is actually what happens in the examined *Re* and Gr_h range. At higher *Re* or lower Gr_h, the Nusselt number would invert the trend described above, increasing in accordance with the Reynolds number [8,9]. Besides, being in a region of thermally developing flow,

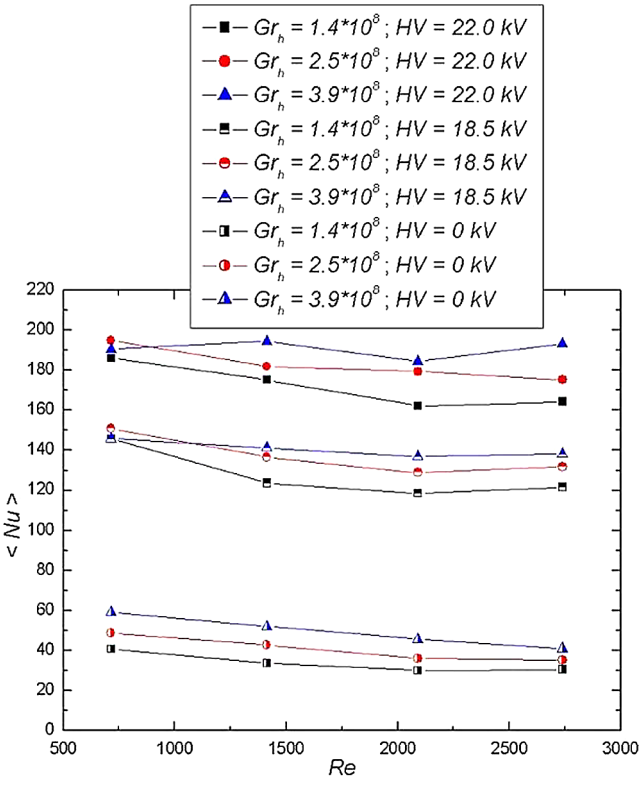

Fig. 3. $\langle Nu \rangle$ vs. *Re* with different Gr_h and *HV* (configuration 1).

the laminarized area may occupy either larger or smaller amounts of the test section, depending on Gr_h and Re. In fact, the local Nusselt numbers were observed to vary non-trivially with the longitudinal position, the heat flux, and the flow rate [10].

When electroconvection is established, heat transfer turns out strongly enhanced, with $\langle Nu \rangle$ at $HV = 22$ kV about 5 times higher. Fig. 3 also shows that $\langle Nu \rangle$ is very sensitive to the applied voltage, while depending only weakly on both Re and Gr_h.

Fig. 4 clearly highlights that the EHD heat transfer augmentation is solely due to the presence of the sharp points. In fact, the Nusselt numbers obtained at $HV = 22$ kV with no points in section C (configuration 2) drop to values comparable to the ones of mixed convection without any applied voltage.

In Fig. 5 $\langle Nu \rangle$ is plotted against Re at $Gr_h = 3.89 \times 10^8$ and $HV = \pm 10$ kV, with the points in configuration 1. The difference in the heat transfer coefficients between the opposite polarities is evident, even at 10 kV.

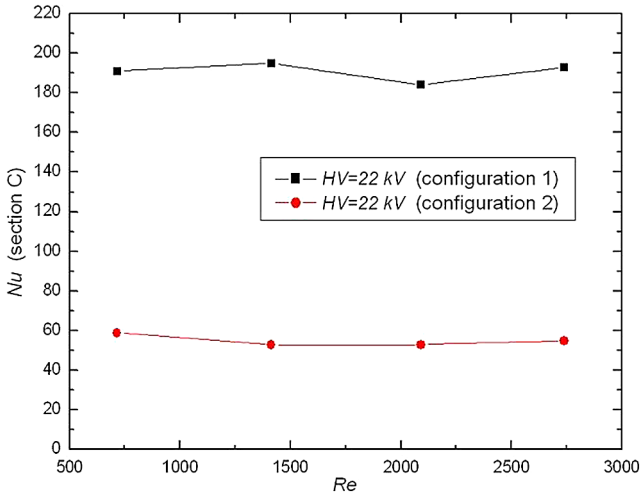

Fig. 4. Nu vs. Re at section C with $Gr_h = 3.89 \times 10^8$ and $HV = 22$ kV (configuration 1 vs. 2).

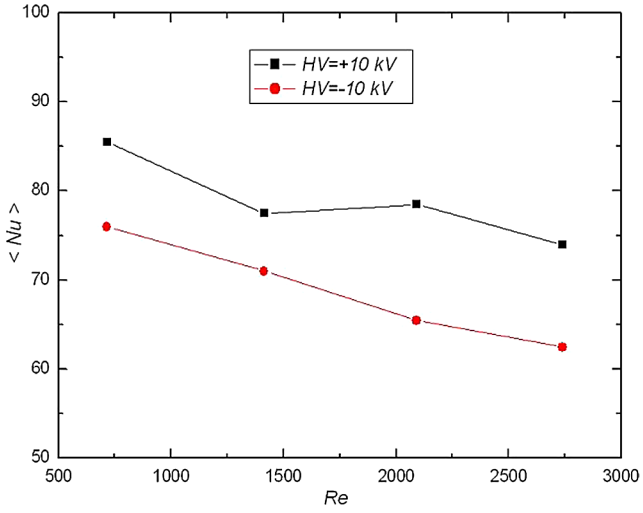

Fig. 5. $\langle Nu \rangle$ vs. Re with $Gr_h = 3.89 \times 10^8$ and $HV = \pm 10$ kV (configuration 1).

As already stressed in the theoretical introduction of this work, the body force responsible for heat transfer enhancement is electrophoresis. However, free charge can build up by three different mechanisms, namely temperature gradients, field-enhanced dissociation, and ion injection.

Convection due to interactions between thermal gradients and electric field (also known as electrothermal convection) is described by the dimensionless number Gr_τ, called the electrophoretic Grashof number:

$$Gr_\tau = \frac{\varepsilon \beta_\tau E^2 (T_{w\_\text{in}} - T_b) D_h^2}{\rho \nu^2} \tag{8}$$

where τ is the free charge relaxation time and $\beta_\tau = -\frac{1}{\tau}\frac{\mathrm{d}\tau}{\mathrm{d}T}$ its temperature coefficient. Being Gr_τ proportional to E^2, electrothermal convection cannot be influenced by the polarity of the electrodes. Also the phenomenon of field-enhanced dissociation of electrolytic species is independent of polarity, being the difference in mobility between positive and negative ions absolutely negligible. Thus, only the ion injection mechanism can explain the results of Fig. 5.

Further tests performed in configuration 2 show that, even at $HV = 10$ kV, the heat transfer coefficients on section A are augmented by placing two additional opposite points 40 mm upstream of the heated region, thus, out of any thermal field in the fluid. Therefore, the observed improvement (see Fig. 6) cannot be ascribed to the interaction between the electric and the thermal fields or, in other words, to an electrothermal convection mechanism.

In conclusion, the results illustrated in Figs. 4–6 are all in favor of the thesis that heat transfer enhancement is due to the flow modification induced by injection of ions at the point electrodes.

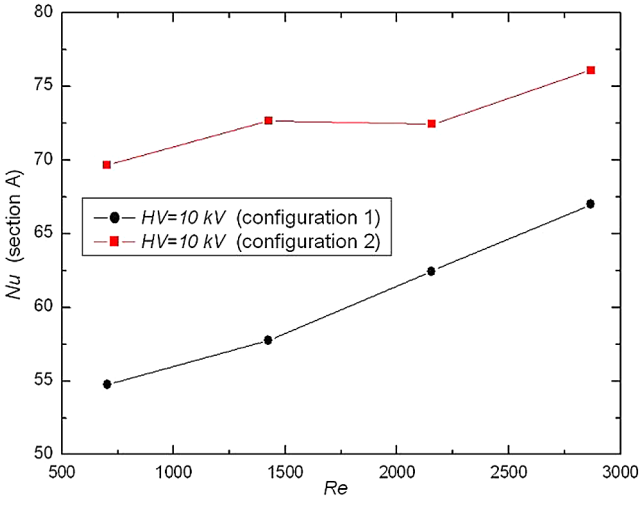

Fig. 6. Nu vs. Re at section A with $Gr_h = 3.89 \times 10^8$ and $HV = 10$ kV (configuration 1 vs. 2).

4. Conclusions

Electrohydrodynamics proved to be a very effective technique of heat transfer augmentation, without significant penalties associated with pressure drop and with a negligible Joule heating. The Nusselt numbers observed at $Re = 700$ in the presence of electroconvection are comparable with the ones obtainable, without the electric field, with a forced flow of $Re = 20\,000$.

With no applied voltage, a regime of turbulent aided mixed convection was established and laminarization effects were observed.

At the application of the electric field, the heat transfer coefficients turned out to be only weakly influenced by the heat flux and the flow rate and could be modulated by varying HV, reaching values up to 5 times higher than the mixed convection ones.

Experimental evidence has been shown that ion injection from the sharp point electrodes, which induces a jet-like motion of cold mass from the center of the duct towards the outer heated wall, is very likely to be the main cause of the measured heat transfer enhancement.

The indications provided by this experimental campaign are encouraging for practical applications, such as size and pumping power reduction of compact heat exchangers. It will be desirable to keep the Reynolds number as low as possible, obtaining laminar flow conditions. In fact, as experimentally proved in [6,11], inducing an EHD secondary flow in the laminar regime does not produce the large pressure drops typical of turbulence.

References

[1] J.A. Stratton, Electromagnetic Theory, McGraw-Hill, New York, 1941, p. 137.
[2] N. Felici, D.C. Conduction in liquid dielectrics—A survey of recent progress (Part I), Direct Current 2 (3) (1971) 90–99.
[3] A. Richter, A. Plettner, K.A. Hotmann, H. Sandmaier, A micromachined electrohydrodynamic (EHD) pump, Sensors and Actuators – A: Phys. 29 (2) (1991) 159–168.
[4] P. Atten, Electrohydrodynamic instability and motion induced by injected space charge in insulating liquids, IEEE Trans. Dielectrics Electrical Insulation 3 (1) (1996) 1–17.
[5] P. Atten, B. Malraison, M. Zahn, Electrohydrodynamic plumes in point-plane geometry, IEEE Trans. Dielectrics Electrical Insulation 4 (6) (1997) 710–718.
[6] J.S. Paschkewitz, D.M. Pratt, The influence of fluid properties on electrohydrodynamic heat transfer enhancement in liquids under viscous and electrically dominated flow conditions, Experimental Thermal Fluid Sci. 21 (2000) 187–197.
[7] B. Metais, E.R.G. Eckert, Forced, mixed, and free convection regimes, J. Heat Transfer – Trans. ASME 86 (1964) 295–296.
[8] T. Aicher, H. Martin, New correlations for mixed turbulent natural and forced convection heat transfer in vertical tubes, Internat. J. Heat Mass Transfer 40 (15) (1997) 3617–3626.
[9] G.P. Celata, F. D'Annibale, A. Chiaradia, M. Cumo, Upflow turbulent mixed convection heat transfer in vertical pipes, Internat. J. Heat Mass Transfer 41 (1998) 4037–4054.
[10] W. Grassi, D. Testi, M. Saputelli, EHD enhanced heat transfer in a vertical annulus, Internat. Commun. Heat Mass Transfer 32 (6) (2005) 748–757.
[11] J.L. Fernández, R. Poulter, Radial mass flow in electrohydrodynamically-enhanced forced heat transfer in tubes, Internat. J. Heat Mass Transfer 30 (10) (1987) 2125–2136.